ISSN NO: 9726-001X
Volume 10 Issue 03 2022

JOURNAL OF CURRENT SCIENCE

Interlaminar shear strength and self-healing of spread carbon fiber/woven carbon fiber hybrid reinforced epoxy resin laminates containing microcapsules

Murthy.S.L, Suresh Patil.G.L, Dr.B.H.Manjunath

Asst. Prof, Assoc. Prof, Prof. & HOD

murthypdit@gmail.com, glspatil@gmail.com, bhmanj@gmail.com

Department of Mechanical, Proudhadevaraya Institute of Technology, Abheraj Baldota Rd, Indiranagar, Hosapete, Karnataka-583225

Abstract

Improving the mechanical characteristics and healing effectiveness of self-healing carbon fibre reinforced polymer (CFRP) using microcapsules (MCs) including healing agents is the goal of this work. Combining spread carbon fibre (SCF) with woven carbon fibre (WCF) is one way to enhance mechanical qualities. The self-healing SCF/WCF hybrid laminates were tested for interlaminar shear strength and healing efficiency using short beam shear tests. The results were compared to those of self-healing SCF/EP and self-healing WCF/EP laminates. In order to assess the microstructure-elastic property relationship, finite element analysis (FEA) was run on SCF/WCF hybrid laminates including MCs using a representative volume element (RVE) model. In addition, we validated the RVE model by comparing analytical and experimental data, and we ran FEAs of short beam shear tests with the elastic parameters predicted by the models. The mechanical characteristics of self-healing CFRP laminates were found to be improved by combining SCF and WCF, according to the testing findings, as compared to self-healing SCF/EP laminates. Due to the presence of substantial transverse fractures in the WCF layers, the self-healing SCF/WCF hybrid laminates were unable to demonstrate enough healing efficiency. Hence, reducing the propagation of the huge fracture in the WCF layer is essential for improving healing efficiency. According to the findings of the analysis, the stress concentration was in the WCF layer and could be reduced by making the SCF layer thicker. Analytical findings and experimental outcomes were highly concordant. The study's RVE model accurately predicted the self-healing CFRP laminates' attributes and offered recommendations for microstructure design to improve mechanical properties and healing efficiency.

Keywords: Short beam shear test, Finite element method, Representative volume element, Composite materials, Spread carbon fiber, Woven carbon fiber, Microcapsule, Interlaminer shear strength, Elastic properties, Self-healing

1. Introduction

Carbon fiber reinforced polymer (CFRP) is a material with superior specific strength and specific stiffness. It is widely used in various fields, including aerospace and automotive industries. However, the complex microstructure of CFRP can cause microscopic damage within the CFRP due to repeated thermal and mechanical loading in service. Accumulation of this damage can lead to sudden failure. Additionally, although the amount of CFRP waste tends to increase every year, most waste is disposed in landfills, which can cause significant environmental issues (Gopalraj and Kärki, 2020; Qureshi, 2022). Researches are being conducted to add a self-healing function to CFRP using microcapsules (MCs) as a solution to these issues.

Microencapsulated healing agents are distributed with catalysts throughout the matrix of CFRP to impart

self-healing function to CFRP. When the self-healing CFRP is damaged, the embedded MCs break and release healing agents. The healing agents flow into the cracks and polymerize upon contact with the embedded catalysts. As a result, the fractured surfaces can be rebonded, thereby preventing crack propagation and fracture. Kessler et al. (2003) first reported on the self-healing of CFRP by incorporating dicyclopentadiene (DCPD) monomer filled urea-formaldehyde MCs and Grubbs' catalyst in woven carbon fiber (WCF)/epoxy resin (EP) laminates. They investigated the healing efficiency on a mode I interlaminar fracture toughness and observed a recovery of over 80 %. Sanada et al. (2006, 2008, 2015) researched on the interfacial debonding of CFRP and proposed self-healing polymer coated fiber strand for unidirectional (UD) CFRP. The self-healing polymer consists of EP containing MCs and Grubbs' catalysts. Tsilimigkra et al. (2020) fabricated self-healing CFRP laminates with only 10 wt% MCs and investigated a mode II interlaminar fracture toughness. The addition of low MC content resulted in a less negative effect on the mechanical properties, and the mode II interlaminar fracture toughness were recovered up to 84 %.

Good dispersion of the MCs in the self-healing CFRPs is needed because it can improve mechanical properties and healing efficiency by alleviating stress concentrations near MCs and delivering sufficient healing agents to extensive damage (Williams et al., 2007; Patel et al., 2010). Previously, we have proposed a self-healing UD CFRPs using the spread carbon fiber (SCF) as the reinforcement and investigated self-healing of interlaminar fracture in the laminates (Sanada et al., 2017; Nassho and Sanada, 2021a; Nassho et al., 2021b). The SCF is made from carbon fiber strands using tow-spreading technology to increase the gaps between fibers (EL-Dessouky and Lawrence, 2013). By using SCF as reinforcement, the MCs enter the gaps, and MC aggregation can be suppressed. In our study, we performed a short beam shear test and found that as the MC diameter and concentration increased, the healing efficiency increased, but the apparent interlaminar shear strength and stiffness decreased (Sanada et al., 2017; Nassho and Sanada, 2021a). Additionally, we fabricated self-healing UD CFRPs with MCs containing healing agents and a UV fluorescent dye, and observed the crack propagation. It was shown that the microstructure of the laminates significantly influences the crack propagation (Nassho et al., 2021b). However, it was difficult to exhibit superior mechanical properties because the self-healing SCF reinforced polymers have low carbon fiber concentration.

Numerical simulations are necessary to understand complex phenomena and obtain design guidelines for improving mechanical properties and healing efficiency of self-healing CFRPs. However, the quantification of CFRP behavior requires extensive experimental and modeling efforts due to their heterogeneous structure, various laminate configurations and anisotropic properties. Multiscale modeling approaches are usually used to simulate CFRPs, thereby saving a lot of time and computational power (Müzel et al., 2020). The behavior of composites can be analyzed at various length scales from micro to macro. Bostanabad et al. (2018) examined the effect of yarn angle, fiber volume fraction and fiber misalignment angle in micro and meso three dimensional (3D) representative volume element (RVE) models on the behavior of macroscale woven CFRP. Their study showed that yarn angle affects the behavior of woven CFRP. Zhang et al. (2022) employed multiscale modeling approach to evaluate the micro and meso 3D RVE models sequentially. They reported that the analytical results of the longitudinal and transverse uniaxial tests were in agreements with the experimental results, and a simplified model of the pressure vessel could predict the burst pressure. Qiaoli et al. (2023) generated a 3D RVE model of micro and meso structures and then analyzed the behavior of plain woven CFRP laminates from a macroscale model under three point bending. The results were in good agreement with the experiments conducted for verification and provided insight into the damage mechanism. Therefore, the RVE modeling approach is effective to be modeled complex microstructures such as CFRP laminates and to predict their properties and behaviors.

The aim of this study is to improve the mechanical properties of self-healing CFRP laminates by hybridizing two types of carbon fibers as reinforcements: SCF and WCF. The use of WCF can increase the overall carbon fiber concentration in the self-healing CFRP laminates, which is expected to improve the mechanical properties (Brunbauer et al., 2015). However, it is not possible to disperse MCs evenly among the fibers of WCF. Therefore, high mechanical properties and healing efficiency can be expected by hybridizing the SCF and the WCF. Figure 1 shows a schematic image of microstructure in the self-healing SCF/WCF hybrid laminates. In addition, since SCF has large gaps between carbon fibers, MCs can be expected to enter the gaps between carbon fibers (Sanada et al., 2017; Nassho and Sanada, 2021a). Using the self-healing method proposed by White et al. (2001), MCs and Grubbs' catalysts were dispersed in the matrix of the laminates. The short beam shear test was conducted on the self-healing CFRP laminates to investigate the effect of the laminate configuration on the mechanical properties and the healing efficiency. The crack propagation and the release of healing agents were also observed by using the MCs containing UV fluorescent dye and healing

agents to examine the relation between the strength recovery and microstructure of the self-healing CFRP laminates. Then, the finite element analysis (FEA) using a 3D RVE models was performed to predict the elastic properties and internal stress of the SCF/WCF hybrid laminates containing MCs. The predicted elastic behaviors were examined in relation to the microstructure of the laminates. We also considered microstructure design guidelines to achieve high mechanical properties and healing efficiency. Then, we performed the FEA of the short beam shear test using the elastic properties predicted from the RVE models and verify the validation of the RVE models by comparing the analytical results with the experimental results.

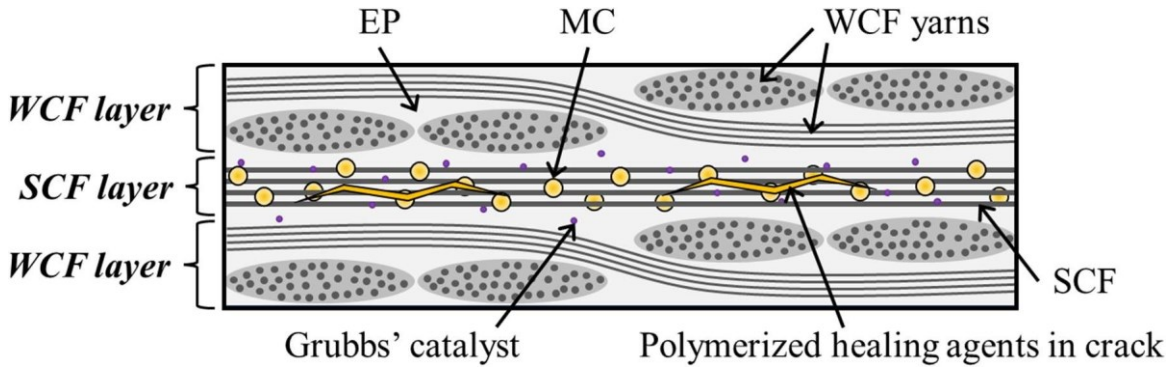

Fig. 1 Schematic image of microstructure in self-healing SCF/WCF hybrid laminates. MCs can be expected to enter the gaps between carbon fibers, because SCF has large gaps between carbon fibers.

2. Experimental methods

2.1 Materials and specimens

2.1.1 Pre-pregs

First, pre-pregs were fabricated: SCF pre-preg and WCF pre-preg. The SCF was prepared for the reinforcement by spreading carbon fiber strands (TORAYCA T700SC-12000, Toray Industries, Inc.) to 40 mm width with a tow-spreading technology (Harmoni Industry Co., Ltd.). For another reinforcement, 2/2 twill WCF (TORAYCA CO6347B, 198 g/m^2, Toray Industries, Inc.) with thickness of 0.22 mm was used. The density of the warp and weft yarns in WCF were both 12.5 threads/25 mm, and one yarn was constructed with 3 K carbon filaments. The SCF and WCF were impregnated with a matrix. The matrix was bisphenol A epoxy resin (jER 828, Mitsubishi Chemical Co.)/tris-2,4,6-dimethylaminoethylphenol (Ancamine K54, Air Products and Chemicals) mixture containing Grubbs' catalysts (Sigma-Aldrich Co. LLC.). The ratio of jER828 and Ancamine K54 was 10:1 in the EP mixture, and 2.5 wt% Grubbs' catalysts to the matrix was used to cure a healing agent. Then, MCs containing a dicyclopentadiene (DCPD) monomer as the healing agent and 10 wt% UV fluorescent dye (Blenny Giken Ltd.) were spread evenly on the surface of pre-pregs. MCs were supplied by Nissei Technica, Co., Ltd. and the mean diameter of MCs was 120 μm. Note that the pre-preg applied to the surface of the laminates did not contain MCs. Table 1 summarizes two types of pre-pregs.

Table 1 Summary of pre-preg types.

Pre-preg type	MC weight (g)	Weight fraction in pre-preg (wt%)		
		MC	Grubbs' catalyst	Carbon fiber
SCF	0, 0.09	0, 20	0, 2.5	18
WCF	0, 0.09	0, 4.1	0, 2.5	41

2.1.2 Laminates

Next, self-healing CFRP laminates were fabricated by using SCF and WCF pre-pregs. The pre-pregs were laminated with the laminate configurations presented in Table 2. In the Table 2, 0 and 0_W indicate SCF and WCF pre-preg, respectively. After being vacuumed for 10 min, the laminate plate was maintained in a hot press at pressure of 0.04 MPa and temperature of 60℃ for 1 h. Then, it was cured in a constant temperature oven at 60℃ for 24 h. It is noted that the compressive strength of MC (103 μm diameter) was 0.141 MPa (Nassho and Sanada, 2021a), and the cross-sectional observation before the test confirmed that the MCs were also not broken. To evaluate the healing

efficiency, we prepared reference CFRP laminates without Grubbs' catalysts using the same procedures as the self-healing CFRP laminates. We also fabricated neat CFRP laminates without MCs and Grubbs' catalysts for comparison. The cured laminates were processed into the shape of short beam specimens according to the JIS K7078 as shown in Fig. 2(a). The h in Fig. 2(a) shows the specimen thickness.

Table 2 Summary of laminate types for reference and self-healing.

Laminate type	Laminate configuration	MC weight in pre-preg (g)		Weight fraction (wt%)	
		SCF pre-preg	WCF pre-preg	MC	Carbon fiber
WE	$[0_w]_8$	-	0.09	4.1	41
SWE1	$[0_w/0/0_w/0/0_w/0/0_w/0/0_w/0/0_w/0/0_w/0/0_w]$	0.09	0	3.4	37
SWE2	$[0_w/0_2/0_w/0_2/0_w/0_2/0_w/0_2/0_w/0_2/0_w/0_2/0_w]$	0.09	0	5.7	35
SWE4	$[0_w/0_4/0_w/0_4/0_w/0_4/0_w/0_4/0_w/0_4/0_w]$	0.09	0	8.7	31
SE	$[0]_{36}$	0.09	-	20	18

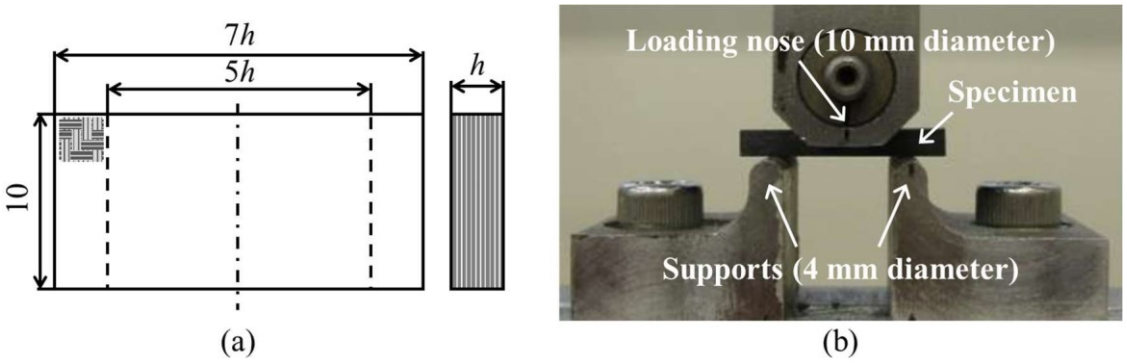

Fig. 2 Short beam shear test: (a) specimen geometry and size (dimensions in mm); (b) setup. The h in Fig. 2(a) shows the specimen thickness. A three-point bending test was conducted with a distance of 5h between supports.

2.2 Short beam shear test

The short beam shear test was performed using a displacement controlled three-point bending test machine (EHF-FB10KN-10LA, Shimadzu Co.) according to the JIS K7078 (Fig. 2(b)). The test was conducted under room temperature at rate of 0.65 mm/min. The virgin test was stopped when the load reached its maximum and began to decrease. The damaged specimen was left at room temperature for 24 h while clamped in a vise. It was then removed from the vise, and the healing agent was cured at 80℃ for 24 h. After healing, the test was repeated. The apparent interlaminar shear strength (τ_c) is obtained with the following equation:

$$\tau_c = \frac{3P_c}{4bh} \quad (1)$$

where P_c is the maximum load obtained in the virgin test, and b is the specimen width.

The healing efficiency (η) was evaluated as follows by using the strain energies of specimens up to displacement at the maximum load during the virgin test.

$$\eta = \frac{U_c^{healed} - U_c^{damaged}}{U_c^{virgin} - U_c^{damaged}} \quad (2)$$

where U_c^{virgin} is the strain energy obtained from the load-displacement curve of self-healing CFRP laminates for the virgin test, U_c^{healed} is the strain energy obtained from the load-displacement curve of self-healing CFRP laminates for the retest after healing, and $U_c^{damaged}$ is the strain energy obtained from the load-displacement curve of reference and

self-healing CFRP laminates for the retest. The detailed description of the healing efficiency evaluation method using strain energy has already been provided in the previous study (Sanada et al., 2017; Nassho and Sanada, 2021a).

The damaged area was observed using an optical microscope (VHX-7000, Keyence Co.) on the specimen after the virgin test. The cross section perpendicular to the longitudinal direction of the specimen was observed under UV light (NSPU510CS, Nichia Co.). Before the short beam shear test, the cross sections of the specimen were polished with distilled water using a waterproof paper.

3. Analytical methods

3.1 RVE models and homogenization

The 3D RVE models were generated by using Digimat-FE (MSC software) to investigate the elastic properties and stress distribution in reference SCF/WCF hybrid laminates as shown in Fig. 3. In the RVE model, a rectangular cartesian coordinate system (x, y, z) was used, and periodic boundary conditions were imposed on all faces. The x axis was assumed to lie along the longitudinal direction of SCF and warp direction of WCF yarn, and the y axis was the transverse direction of SCF and weft direction of WCF yarn, and the z axis was assumed to lie along thickness direction of the reference SCF/WCF hybrid laminates.

In the RVE model of reference SCF/WCF hybrid laminates, two layers were constructed: the SCF layer and the WCF layer. The WCF layer consists of EP as the matrix and 2/2 twill WCF as the reinforcement. Note that the warp and weft yarns of the WCF were homogenized composites of carbon fiber and EP as an elastic and transversely isotropic material, and the dimensions were based on the actual yarns with a cross section of 1.9 mm width and 0.144 mm thickness. Assuming the laminate configurations of SWE1, SWE2 and SWE4 used in the experiment, the thickness of the SCF layer (t) was varied to 0.1, 0.2 and 0.4 mm, respectively, to investigate the effect of the laminate configuration on the elastic properties and stress distribution of the reference SCF/WCF hybrid laminates. The SCF layer was modeled as a homogenized MC/SCF/EP composites with a homogeneous, elastic and transversely isotropic material using the values predicted by the RVE model of the MC/SCF/EP composites. The RVE model of the MC/SCF/EP composites represents the SCF pre-preg described in Section 2.1, assuming 20 wt% MCs and 18 wt% carbon fibers. The MCs were homogenized as the spherical isotropic inclusions having negligible Young's modulus and incompressible because polymeric shell of actual MC is very thin (Ahmed et al., 2018). The elastic properties of the homogenized SCF/EP composites in the RVE model of the MC/SCF/EP composites were calculated using the RVE model of the SCF/EP composites. The RVE model of the SCF/EP composites consisted of EP and carbon fiber oriented in the x direction. It is assumed that the inclusions (carbon fiber and MC) and the matrix are perfect bonding, with the restriction that the inclusions cannot overlap each other.

We applied the automatic property evaluation function implemented in the Digimat-FE software, which uses the finite element solver of the Marc software to predict the elastic properties of the RVE models. The RVE model of the reference SCF/WCF hybrid laminates was meshed using voxel elements, while the RVE models of the MC/SCF/EP composites and SCF/EP composites were meshed using tetrahedral elements. The elastic properties of homogenized SCF/EP composites were first predicted by using the RVE models of SCF/EP composites. Then, we predicted the elastic properties of homogenized MC/SCF/EP composites by the RVE models of MC/SCF/EP composites. The elastic properties of constituent materials used in this study were shown in Table 3 (Daniel and Ishai, 2006; Rzeszutko et al., 2003; Epoxy Technology, 2011). Note that carbon fiber was assumed to be an isotropic material in this study. Table 4 summarized the predicted elastic properties of the homogenized composites using the values in Table 3 and the RVE models of the MC/SCF/EP and SCF/EP composites shown in Fig. 3. Then, the elastic properties of the RVE models of reference SCF/WCF hybrid laminates were predicted by using the predicted elastic properties of the homogenized MC/SCF/EP composites. In addition, the internal stress state in the RVE model of the reference SCF/WCF hybrid laminates was also evaluated by imposing 1 % shear strain in the x-z plane.

ISSN NO: 9726-001X
Volume 10 Issue 03 2022

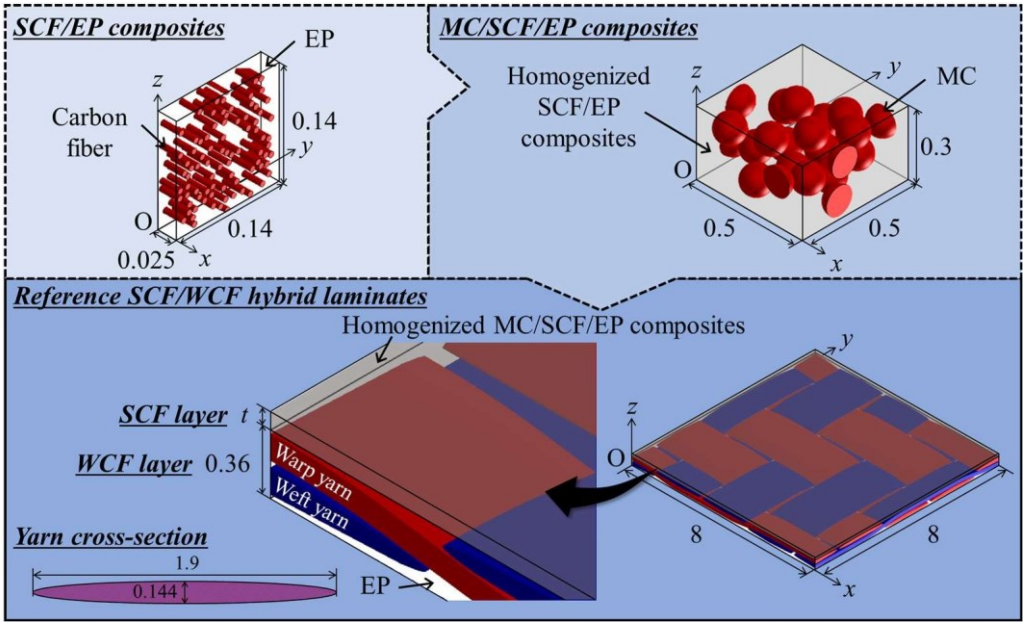

Fig. 3 Schematic image of the RVE model of reference SCF/WCF hybrid laminates (dimensions in mm). The complex microstructure of reference SCF/WCF hybrid laminates was modeled using homogenization.

Table 3 Elastic properties of constituent materials in RVE models.

Constituent material	Young's modulus (GPa)	Poisson's ratio
MC	10^{-6}	0.49
Carbon fiber	230	0.2
EP	3.4	0.3

Table 4 Predicted elastic properties of the homogenized composites.

Homogenized composites	Young's moduli (GPa)		Shear modulus (GPa)	Poisson's ratios	
	E_x^H	E_y^H	G_{xy}^H	ν_{xy}^H	ν_{yz}^H
SCF/EP	37.7	4.80	1.80	0.279	0.394
MC/SCF/EP	18.4	2.97	1.17	0.270	0.348

3.2 Short beam specimen model

The two-dimensional (2D) short beam specimen model with the assumption of plane strain was analyzed by using the ANSYS FEA code to obtain the load-displacement curves. The validation of the RVE models in Section 3.1 was verified by comparing the analytical curves with the experimental curves. The geometry, size and boundary conditions were shown in Fig. 4, due to symmetry in both geometry and loading configurations, only one-half of the short beam specimens were modeled. The geometry and size of the short beam specimen model were based on those of the representative short beam specimen used in the experiments. The x axis was assumed to lie along the longitudinal direction of SCF and warp direction of WCF yarn, and the z axis was thickness direction of the reference SCF/WCF hybrid laminates. The PLANE183 element was used to mesh the short beam specimen models. The elastic properties of the short beam specimen model were based on the predicted values from the RVE model of the reference SCF/WCF hybrid laminates. The fixtures consisting loading nose and support were modeled as steel. The compressive load was applied to the loading nose up to the maximum load value of the short beam shear test obtained from the experiments. The penalty function method was used to simulate contact between the specimen and the fixtures.

ISSN NO: 9726-001X
Volume 10 Issue 03 2022

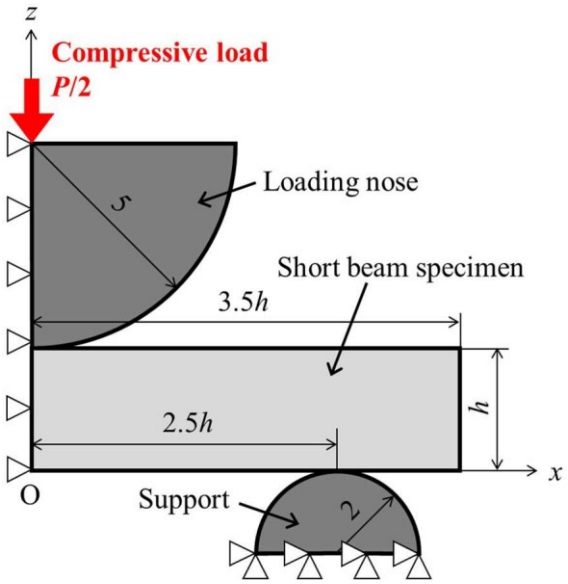

Fig. 4 Geometry, size and boundary conditions for the 2D short beam specimen model (dimensions in mm). The model assumed that the longitudinal and thickness direction of short beam specimen was along the *x* axis and *z* axis, respectively.

4. Results and discussion

4.1 Load-displacement curves

The short beam shear tests of reference and self-healing CFRP laminates were performed to evaluate the apparent interlaminar shear strength and the healing efficiency. Figure 5 shows the typical load-displacement curves of reference and self-healing CFRP laminates obtained from virgin test and retest for SWE2. The healed loading curve for self-healing CFRP laminates initially matched the virgin loading curve. This indicates that the damage has healed. Similar tendencies were observed in other laminate types. The self-healing CFRP laminates shown in Fig. 5(b) exhibited the apparent interlaminar shear strength of 42 MPa and the healing efficiency of 28 %, as calculated from Eq. (1) and Eq. (2).

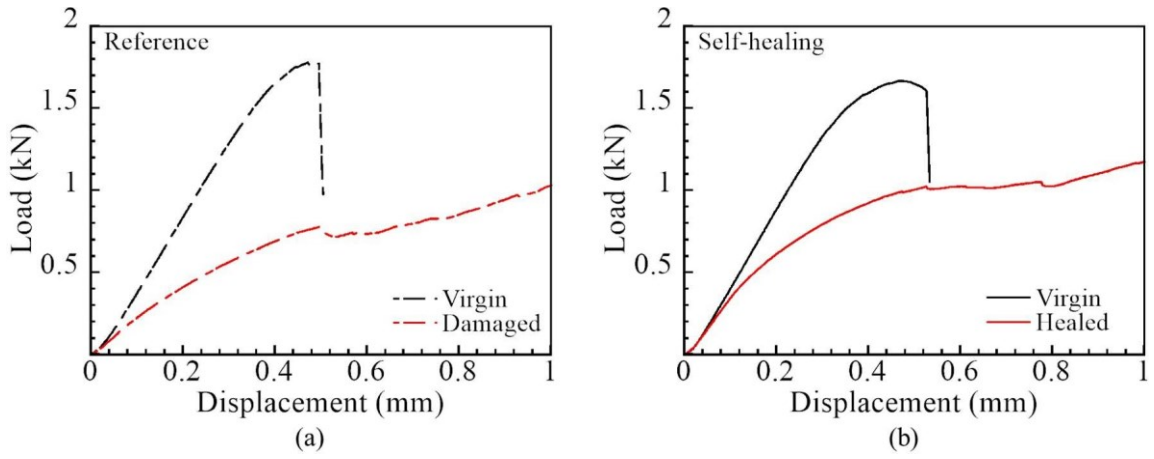

Fig. 5 Typical load-displacement curves of SWE2: (a) reference CFRP laminates; (b) self-healing CFRP laminates. Self-healing CFRP laminates showed a recovery of stiffness and strength compared to reference CFRP laminates.

4.2 Effect of MC inclusion on mechanical properties

Figure 6 shows the apparent shear stress-displacement curves obtained from the virgin test of neat and self-healing CFRP laminates. The vertical axis in Fig. 6 represents the apparent shear stress obtained from Eq. (1), and the initial

ISSN NO: 9726-001X
Volume 10 Issue 03 2022

slope of the apparent shear stress-displacement curve is related to the stiffness of the specimen. For both neat and self-healing CFRP laminates, the initial slope of the curves decreased, and the stiffness decreased as the number of SCF layers increased. This is due to the lower carbon fiber content in the SCF layer compared to the WCF layer, and the overall carbon fiber content decreased as the number of SCF layers increased. For the neat CFRP laminates, the apparent shear stress-displacement curves were linear up to near the peak shear stress and then dropped rapidly. With the exception of neat SE, these neat CFRP laminates exhibited cracks at near the loading nose, transverse cracks and delamination. The neat SE showed flexural fracture peculiar to laminates using SCFs (EL-Dessouky and Lawrence, 2013). Note that the apparent interlaminar shear strength of the laminates that exhibited flexural fracture is not valid in accordance with the JIS K7078 standard, but it was adopted in this study for comparison with the apparent interlaminar shear strength of other laminates. On the other hand, the self-healing CFRP laminates showed lower stiffness, and nonlinear behavior near the peak shear stress compared to the curves of neat CFRP laminates. These could be due to the lower stiffness of MCs compared to that of EP matrix, and the increased virgin fracture toughness of EP matrix by containing MCs (Brown et al., 2004). In addition, for self-healing CFRP laminates, the behavior of the apparent shear stress-displacement curves varied with the laminate configuration. The behavior of the curves for self-healing SWE1 and SWE2 was similar to that for self-healing WE and brittle, while the curve for self-healing SWE4 decreased slowly after the peak shear stress, similar to that for self-healing SE with ductile behavior. Cracks at near the loading nose and transverse cracks were also observed in the self-healing WE and SWE, as discussed below in Section 4.3. Moreover, as the number of SCF layers increased, more cracks along the MCs were observed in these self-healing CFRP laminates.

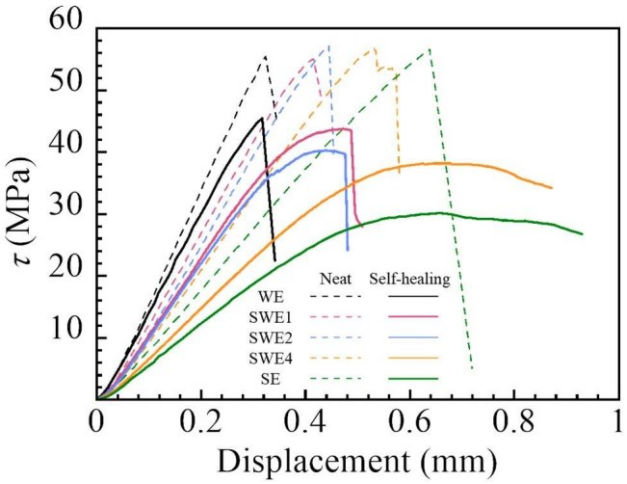

Fig. 6 Typical apparent shear stress-displacement curves for neat and self-healing CFRP laminates with different laminate configuration. The self-healing CFRP laminates showed lower stiffness and nonlinear behavior compared to the neat CFRP laminates, but the stiffness increased as the number of SCF layers decreased.

Figure 7 presents the apparent interlaminar shear strength of neat and self-healing CFRP laminates, along with the reduction ratio of the apparent interlaminar shear strength caused by the inclusion of MCs and Grubbs' catalysts. Regardless of the change in the laminate configuration, the apparent interlaminar shear strength of neat CFRP laminates was almost the same. This may be because the apparent interlaminar shear strength of the laminates is highly dependent on the properties of the matrix. The inclusion of MCs and Grubbs' catalysts reduced the apparent interlaminar shear strength for all laminate configurations. However, for the self-healing CFRP laminates, the apparent interlaminar shear strength and the strength reduction ratio tended to improve as the SCF layer decreased. This could be attributed to the lower concentration of MCs with low strength and higher concentration of carbon fibers. Therefore, the hybridization of SCF and WCF can improve the stiffness and apparent interlaminar shear strength compared to self-healing SE. In particular, self-healing SWE can exhibit the apparent interlaminar shear strength as high as WE.

ISSN NO: 9726-001X
Volume 10 Issue 03 2022

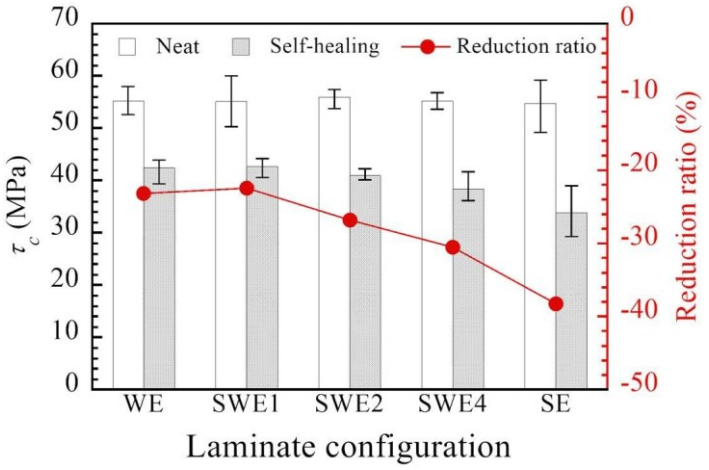

Fig. 7 Effect of laminate configuration on the apparent interlaminar shear strength of neat and self-healing CFRP laminates and the strength reduction ratio. The self-healing CFRP laminates showed lower apparent interlaminar shear strength compared to the neat CFRP laminates, but the strength reduction ratio improved as the number of SCF layers decreased.

4.3 Effect of laminate configuration on strength recovery

Figure 8 shows the effect of laminate configuration on the apparent interlaminar shear strength and the healing efficiency for self-healing CFRP laminates. As we previously mentioned, the apparent interlaminar shear strength of WE and SWE was higher than that of SE. However, the healing efficiency of WE and SWE was significantly lower than that of SE. The healing efficiency of SWE also tended to increase slightly as the number of SCF layers between the WCF layers increased. This could be because the number of broken MCs increased as the number of SCF layers increased, thereby releasing sufficient healing agents into the crack.

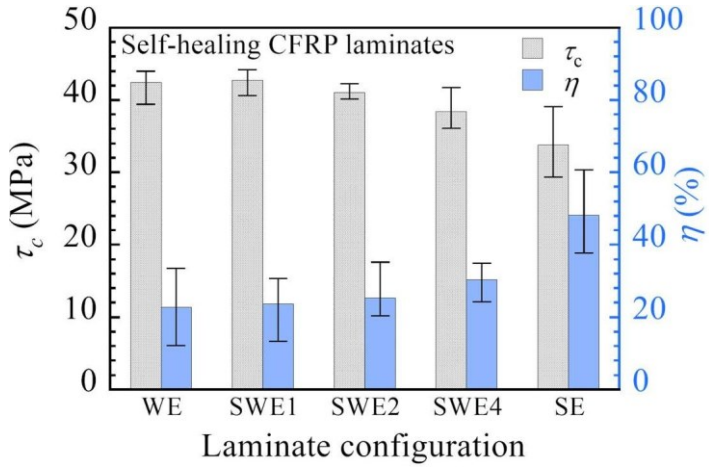

Fig. 8 Effect of laminate configuration on the apparent interlaminar shear strength and the healing efficiency of self-healing CFRP laminates. The healing efficiency of the laminates increased as the number of SCF layers increased.

Figure 9 shows the damaged area of the self-healing CFRP laminates after the virgin test. The upper figures in Fig. 9 show the observation without UV irradiation, while the lower figures show the observation with UV irradiation. It is possible to visually confirm that the healing agents have flowed out into the crack, because they cause healing agents containing the UV fluorescent dye to glow blue, when observed under UV light. In the case of the SE, cracks propagated in the fiber direction and broke the many MCs. Under UV light, the healing agents showed strong luminescence, indicating sufficient penetration into the cracks. Therefore, it is thought that the SE showed the highest healing efficiency. However, many large transverse cracks were generated in the WCF layer for the WE, and these cracks progressed along the fiber interface. When observed under UV light, the luminescence was weak, and the

ISSN NO: 9726-001X
Volume 10 Issue 03 2022

healing agents were unable to penetrate into the cracks. Therefore, it is believed that the WE showed the lowest healing efficiency. Moreover, the SWE had transverse cracks similar to those observed in the WE, but the cracks in SWE2 and SWE4 were relatively small and propagated along the MCs compared to the WE. Under UV light observation, the healing agents exhibited strong luminescence, confirming their penetration into the cracks. Therefore, it is considered that the SWE has higher healing efficiency than the WE.

The experiments confirmed that the self-healing SCF/WCF hybrid laminates had superior mechanical properties. However, the healing efficiency of the laminates was challenged due to the generation of large transverse cracks in the WCF layers.

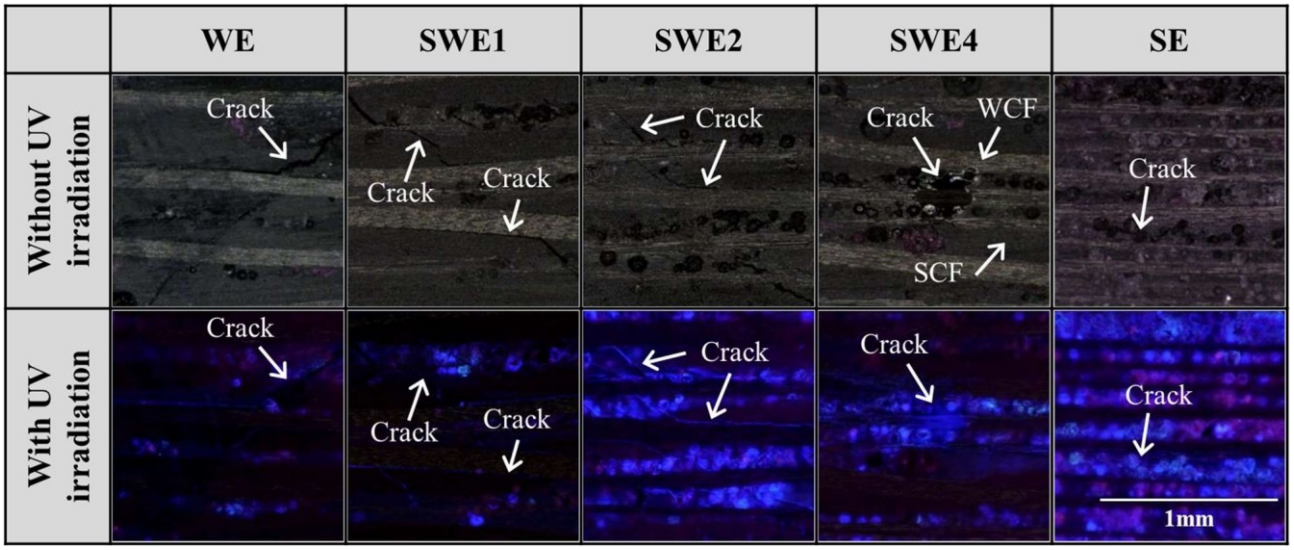

Fig. 9 Optical micrographs of damaged area of self-healing CFRP laminates with different laminate configuration after virgin test. For SWE2, SWE4 and SE, the healing agents exhibited strong blue luminescence when observed under UV irradiation, thereby confirming penetration of healing agents into the cracks.

4.4 Predicted elastic behaviors from RVE models of SCF/WCF hybrid laminates containing MCs

The FEA using the RVE models was performed to predict the elastic properties and internal stress of the reference SCF/WCF hybrid laminates. Considering the laminate configurations of the reference SWE used in the experiment, the thickness of the SCF layer was varied, to examine the effect of the laminate configuration on the elastic behaviors. Figure 10 presents the effect of laminate configuration on the predicted elastic properties from the RVE models of the reference SCF/WCF hybrid laminates. The Young's moduli (E_x^C, E_y^C, E_z^C), shear moduli (G_{yz}^C, G_{zx}^C, G_{xy}^C) and Poisson's ratios (ν_{xy}^C, ν_{xz}^C, ν_{zy}^C) were evaluated. As the thickness of the SCF layer increased, the predicted Young's moduli and shear moduli decreased. The Poisson's ratios were almost constant for laminate configurations. The focus on the shear modulus (G_{zx}^C) to consider the short beam shear test showed a similar trend to the experimental results.

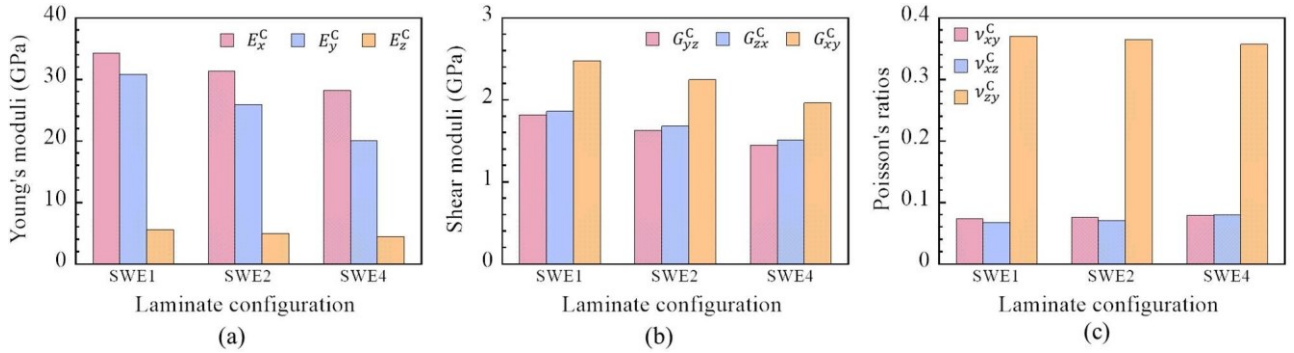

Fig. 10 Effect of laminate configuration on the predicted elastic properties from the RVE models of reference SCF/WCF hybrid laminates: (a) Young's moduli; (b) shear moduli; (c) Poisson's ratios. The predicted shear modulus (G_{zx}^C) decreased as the thickness of SCF layers increased, and exhibited similar trend to the experimental results.

ISSN NO: 9726-001X
Volume 10 Issue 03 2022

The shear stress (τ_{zx}) distribution near the origin of the RVE model was evaluated by imposing 1 % shear strain in the *x*-*z* plane as shown in Fig. 11. The dashed line in Fig. 11 indicates the interface between the SCF layer and the WCF layer. Note that in this study, crack propagation behavior cannot be predicted. However, the location of the stress concentration can be predicted to be the initial point of damage in the laminates. High shear stress was observed in the 45° direction along the warp yarn in the WCF layer. Thus, the analytical results confirmed that cracks are likely to occur in the WCF layer. As shown in Fig. 9, transverse cracks occurred in the WCF layer for the experiment of the SWE, and the similar trend was obtained from the analysis results.

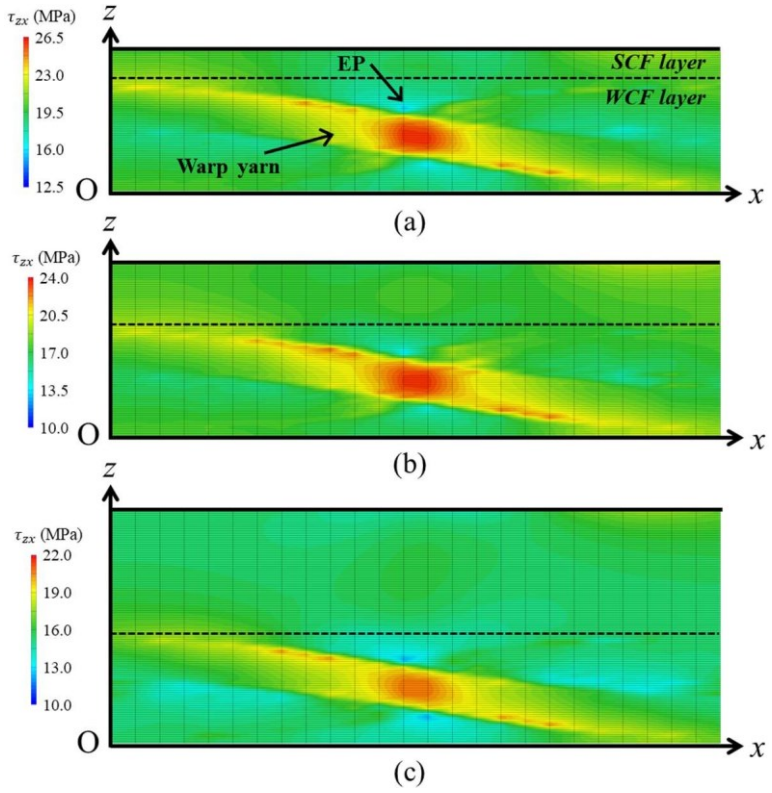

Fig. 11 Shear stress distribution in RVE models of reference SCF/WCF hybrid laminates at shear strain value of 1 %: (a) SWE1; (b) SWE2; (c) SWE4. High shear stress was observed in the WCF layer.

Figure 12 shows the shear stress distribution curves obtained from the RVE models shown in Fig. 11 at the shear strain value of 1 %. Note that the peak of the curve indicates the shear stress most likely to occur. As the thickness of the SCF layer increased, the shear stress distribution curves shifted to the left, and the maximum shear stress, the average shear stress and the shear stress at the peak of the distribution curve extracted from the shear stress distribution curves of the RVE models decreased. This indicates that the SCF layer may be expected to function as a stress relaxation layer for the WCF layer. Therefore, it is considered that by increasing the number of the SCF layer, the stress concentration in the self-healing SCF/WCF hybrid laminates can be reduced, and large transverse cracks can be suppressed.

ISSN NO: 9726-001X
Volume 10 Issue 03 2022

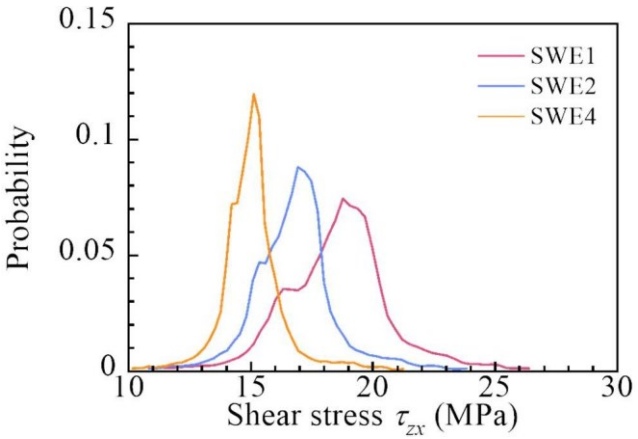

Fig. 12 Shear stress distribution curves in the RVE models of reference SCF/WCF hybrid laminates at shear strain value of 1 %. The shear stress distribution curves shifted to the left as the thickness of the SCF layers increased.

4.5 Comparison of experimental and analytical results

Then, the FEA of the short beam shear test was conducted using the elastic properties predicted from the RVE models to verify the validation of the RVE model. The analytical apparent shear stress-displacement curves obtained from the short beam specimen model having the elastic properties in the RVE models of reference SCF/WCF hybrid laminates were compared with the experimental apparent shear stress-displacement curves as shown in Fig. 13. The analytical results were in good agreement with the experimental results on the initial slopes of apparent shear stress-displacement curves. Figure 14 shows analytical and experimental apparent interlaminar shear strength. Note that stress concentration occurred at near loading nose and support, but the local maximum shear stress generated in the neutral plane of the specimen when the maximum load was applied was defined as the analytical apparent interlaminar shear strength. Although the analytical results slightly decreased compared to the experimental results for all laminate configurations, the difference between the analytical and experimental apparent interlaminar shear strength was very small. Therefore, the RVE model in this study can be effective to predict the mechanical properties of the hybrid SCF/WCF laminates containing MCs.

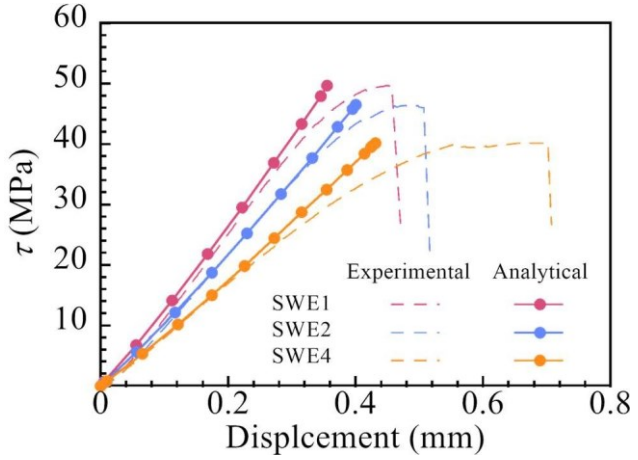

Fig. 13 Analytical and experimental apparent shear stress-displacement curves for short beam specimens of reference SCF/WCF hybrid laminates. The initial slopes of the analytical curves were in good agreement with those of the experimental curves.

ISSN NO: 9726-001X
Volume 10 Issue 03 2022

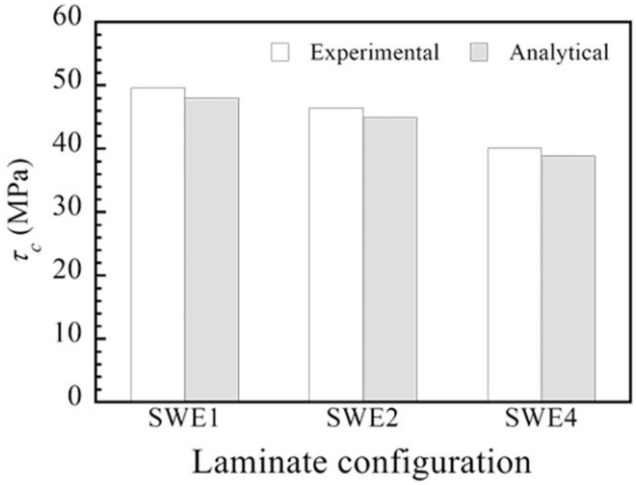

Fig. 14 Comparison of apparent interlaminar shear strength obtained from analytical and experimental short beam specimens of reference SCF/WCF hybrid laminates. The difference between the analytical and experimental results was very small.

5. Conclusions

We investigated the impact of laminate arrangement on mechanical characteristics and healing efficiency by conducting a short beam shear test on self-healing CFRP laminates reinforced with SCF and WCF. Results showed that adding MCs to any laminate configuration reduced the laminates' apparent interlaminar shear strength and stiffness; however, the self-healing SCF/WCF hybrid laminates (SWE) had a smaller strength reduction ratio than the self-healing UD SCF/EP laminates (SE). Hybrid self-healing SCF/WCF laminates outperformed their UD SCF/EP counterparts in terms of stiffness and apparent interlaminar shear strength. As a result, it became clear that self-healing UD SCF/EP laminates may benefit from improved mechanical characteristics via the hybridisation of SCF and WCF. The SCF/WCF hybrid laminates that self-healed, however, were not as effective in the healing process. Big transverse fissures in the WCF layer were found in the self-healing SCF/WCF hybrid laminates, and the damaged spots were visible. Because the healing chemicals could not be released via the huge transverse breaches in the WCF layer, the MCs remained intact. As a result, the self-healing SCF/WCF hybrid laminates' healing efficiency is thought to have diminished. Suppressing the huge transverse fracture in the WCF layer is crucial to increase the healing efficiency.
Hybridising SCF and WCF improved mechanical characteristics, although self-healing SCF/WCF hybrid laminates still need to be made more efficient healers. In order to achieve better mechanical properties and healing efficiency, we analysed the microstructure design guidelines for SCF/WCF hybrid laminates with MCs by modelling them and then evaluating their internal stress and elastic characteristics. The analytical findings corroborated the experimental data, showing that the WCF layer was a hotspot for stress concentration and a potential cracking point. With increasing SCF layer thickness, the shear stress in the RVE model of MC-containing SCF/WCF hybrid laminates also dropped. In self-healing SCF/WCF hybrid laminates, it was shown that increasing the number of SCF layers may lower stress concentration and inhibit significant transverse fractures. Next, we validated the RVE models using FEA by doing a brief beam shear test. The experimental and analytical shear stress-displacement curves agreed well. Hence, our study's RVE model may help get microstructure design recommendations by efficiently predicting the mechanical characteristics of SCF/WCF hybrid laminates including MCs.

References

Ahmed, A., Sanada, K., Fanni, M. and El-Moneim, A. A., A practical methodology for modeling and verification of self-healing microcapsules-based composites elasticity, Composite Structures, Vol.184 (2018), pp.1092-1098.

Bostanabad, R., Liang, B., Gao, J., Liu, W. K., Cao, J., Zeng, D., Su, X., Xu, H., Li, Y. and Chen, W., Uncertainty quantification in multiscale simulation of woven fiber composites, Computer Methods in Applied Mechanics and Engineering, Vol.338 (2018), pp.506-532.

Brown, E.N., White, S.R. and Sottos, N.R., Microcapsule induced toughening in a self-healing polymer composite, Journal of Materials Science, Vol.39 (2004), pp.1703-1710.

Brunbauer, J., Stadler, H. and Pinter, G., Mechanical properties, fatigue damage and microstructure of carbon/epoxy laminates depending on fibre volume content, International Journal of Fatigue, Vol.70 (2015), pp.85-92.

Daniel, I.M. and Ishai, O., Engineering mechanics of composite materials, 2nd ed, Oxford University Press, (2006), p. 375.

EL-Dessouky, H. M. and Lawrence, C. A., Ultra-lightweight carbon fibre/thermoplastic composite material using spread tow technology, Composites Part B: Engineering, Vol.50 (2013), pp.91-97.

Epoxy Technology Inc., Understanding mechanical properties of epoxies for modeling, finite element analysis (FEA), Tech Tip 19, (2011).

Gopalraj, S. K. and Kärki, T., A review on the recycling of waste carbon fibre/glass fibre-reinforced composites: fibre recovery, properties and life-cycle analysis, SN Applied Sciences, Vol.2 (2020), pp.1-21.

Japanese Standards Association, JIS K7078: Testing method for apparent interlaminar shear strength of carbon fiber reinforced plastics by three point loading method, JIS Handbook 72 Kikai Anzen, (2018), pp.104-169 (in Japanese).

Kessler, M. R., Sottos, N. R. and White, S. R., Self-healing structural composite materials, Composites Part A: Applied Science and Manufacturing, Vol.34 (2003), pp.743-753.

Müzel, S. D., Bonhin, E. P., Guimarães, N. M. and Guidi, E. S., Application of the finite element method in the analysis of composite materials: A review, Polymers, Vol.12 (2020), DOI:10.3390/polym12040818.

Nassho, Y. and Sanada, K., Microstructure optimizations for improving interlaminar shear strength and self-healing efficiency of spread carbon fiber/epoxy laminates containing microcapsules, Journal of Composite Materials, Vol.55 (2021a), pp.27-38.

Nassho, Y., Hirooka, S. and Sanada, K., Visualization and self-healing of damage in spread carbon fiber/epoxy laminates containing microcapsules, Journal of the Society of Materials Science, Japan, Vol.70 (2021b), pp.457-464 (in Japanese).

Patel, A. J., Sottos, N. R., Wetzel, E. D. and White, S. R., Autonomic healing of low-velocity impact damage in fiber-reinforced composites, Composites Part A: Applied Science and Manufacturing, Vol.41 (2010), pp.360-368.

Qiaoli, Z., Yuliang, H., Weihan, W., Yutong, L. and Cheng, L., Experimental and numerical investigation of mechanical behavior of plain woven CFRP composites subjected to three-point bending, Chinese Journal of Aeronautics, Vol.36 (2023), pp.505-517.

Qureshi, J., A review of recycling methods for fibre reinforced polymer composites, Sustainability Vol.14 (2022), DOI:10.3390/su142416855.

Rzeszutko, A. A., Brown, E. N. and Sottos, N. R., Tensile properties of self-healing epoxy, TAM Tech Report, (2003), pp.1041-1055.

Sanada, K., Itaya, N. and Shindo, Y., Self-healing of interfacial debonding in fiber-reinforced polymers and effect of microstructure on strength recovery, The Open Mechanical Engineering Journal, Vol.14 (2008), pp.97-103.

Sanada, K., Mizuno, Y. and Shindo, Y., Damage progression and notched strength recovery of fiber-reinforced polymers encompassing self-healing of interfacial debonding, Journal of Composite Materials, Vol.49 (2015), pp.1765-1776.

Sanada, K., Suyama, T. and Nassho, Y., Interlaminar shear strength and self-healing of spread carbon fiber/epoxy laminates containing microcapsules, Journal of the Society of Materials Science, Japan, Vol.66 (2017), pp.299-305 (in Japanese).

Sanada, K., Yasuda, I. and Shindo, Y., Transverse tensile strength of unidirectional fibre-reinforced polymers and self-healing of interfacial debonding, Plastics, Rubber and Composites, Vol.35 (2006), pp.67-72.

Tsilimigkra, X., Bekas, D., Kosarli, M., Tsantzalis, S., Paipetis, A. and Kostopoulos, V., Mechanical properties assessment of low-content capsule-based self-healing structural composites, Applied Sciences, Vol.10 (2020) DOI:10.3390/app10175739.

White, S. R., Sottos, N. R., Geubelle, P. H., Moore, J. S., Kessler, M. R., Sriram, S. R., Brown, E. N. and Viswanathan, S., Autonomic healing of polymer composites, Nature, Vol.409 (2001), pp.794-797.

Williams, G. J., Trask, R. S. and Bond, I. P., A self-healing carbon fibre reinforced polymer for aerospace applications, Composites Part A: Applied Science and Manufacturing, Vol.38 (2007), pp.1525-1532.

Zhang, N., Gao, S., Song, M., Chen, Y., Zhao, X., Liang, J. and Feng, J., A multiscale study of CFRP based on asymptotic homogenization with application to mechanical analysis of composite pressure vessels, Polymers, Vol.14 (2022), DOI:10.3390/polym14142817.